

Structure and properties of sintered MM–Fe–B magnets

R. X. Shang, J. F. Xiong, R. Li, W. L. Zuo, J. Zhang, T. Y. Zhao, R. J. Chen, J. R. Sun, and B. G. Shen

Citation: *AIP Advances* **7**, 056215 (2017);

View online: <https://doi.org/10.1063/1.4973603>

View Table of Contents: <http://aip.scitation.org/toc/adv/7/5>

Published by the [American Institute of Physics](#)

Articles you may be interested in

[Magnetic properties of \(misch metal, Nd\)-Fe-B melt-spun magnets](#)

AIP Advances **7**, 056207 (2017); 10.1063/1.4973846

[Micromagnetic simulation of the influence of grain boundary on cerium substituted Nd-Fe-B magnets](#)

AIP Advances **7**, 056201 (2016); 10.1063/1.4972803

[Coercivity of Nd-Fe-B hot-deformed magnets produced by the spark plasma sintering method](#)

AIP Advances **7**, 056205 (2016); 10.1063/1.4973438

[The magnetic properties of \$\text{MMCo}_5\$ \(MM=Mischmetal\) nanoflakes prepared by multistep \(three steps\) surfactant-assisted ball milling](#)

AIP Advances **7**, 056203 (2016); 10.1063/1.4973395

[Magnetic properties of Sm-Fe-N bulk magnets produced from Cu-plated Sm-Fe-N powder](#)

AIP Advances **7**, 056204 (2016); 10.1063/1.4973396

[Variation of coercivity with Ce content in \$\(\text{Pr,Nd,Ce}\)_2\text{Fe}_{14}\text{B}\$ sintered magnets](#)

AIP Advances **7**, 056228 (2017); 10.1063/1.4977722

HAVE YOU HEARD?

Employers hiring scientists and
engineers trust

PHYSICS TODAY | JOBS

www.physicstoday.org/jobs



Structure and properties of sintered MM–Fe–B magnets

R. X. Shang,^{1,2} J. F. Xiong,^{1,2} R. Li,^{1,2} W. L. Zuo,^{1,2} J. Zhang,^{1,2} T. Y. Zhao,^{1,2}
 R. J. Chen,^{2,3} J. R. Sun,^{1,2} and B. G. Shen^{1,2,a}

¹State Key Laboratory of Magnetism, Institute of Physics, Chinese Academy of Sciences, Beijing 100190, P. R. China

²University of Chinese Academy of Sciences, Beijing 100049, P. R. China

³Key Laboratory of Magnetic Materials and Devices, Ningbo Institute of Materials Technology and Engineering, Chinese Academy of Sciences, Ningbo 315201, P. R. China

(Presented 1 November 2016; received 23 September 2016; accepted 19 October 2016; published online 12 January 2017)

MM₁₄Fe_{79.9}B_{6.1} magnets were prepared by conventional sintering method. The Curie temperature of the sintered MM₂Fe₁₄B magnet was about 210 °C. When the sintering temperature increased from 1010 °C to 1030 °C, the density of the magnet increased from 6.85 g/cm³ to 7.52 g/cm³. After the first stage tempering at 900 °C, the $(BH)_{\max}$ and H_{cj} had a slight increase. The maximum value of $(BH)_{\max} = 7.6$ MGOe and $H_{\text{cj}} = 1080$ Oe was obtained when sintered at 1010 °C and tempering at 900 °C, respectively. The grain size grew very large when the sintering temperature increased to 1050 °C, and the magnetic properties deteriorated rapidly. La reduced by ~ 7.5 at. % in grains, which is almost equal to the increased percentage of Nd. That is mainly because La-Fe-B is very difficult to form the 2: 14: 1 phase. © 2017 Author(s). All article content, except where otherwise noted, is licensed under a Creative Commons Attribution (CC BY) license (<http://creativecommons.org/licenses/by/4.0/>). [<http://dx.doi.org/10.1063/1.4973603>]

I. INTRODUCTION

Due to the higher price and less abundance of Nd, using low-cost and higher abundance of La, Ce partial substitution of Nd in NdFeB has become a hot topic in the study of rare earth permanent magnet in recent years.^{1–3} MM don't need the separation of La, Ce, Pr and Nd elements, which saves more cost (MM = misch metal, consisting of 28.0 at. % La, 52.0 at. % Ce, 5.1 at. % Pr, 14.7 at. % Nd, others 0.2 at. %). Gong *et al.* deem that MM-Fe-B magnets may allow the production with maximum energy product $(BH)_{\max}$ in the range of 10–20 MGOe.⁴ According to the literatures, the $(BH)_{\max}$ of Ba-ferrite and Sr-ferrite is about 5 MGOe, rare earth permanent magnet is in the range of 14~60 MGOe.^{5–8} Therefore, MMFeB magnets may fill the vacancy of $(BH)_{\max}$ between ferrite and NdFeB.

In the work by Ko, *et al.* the $(BH)_{\max} = 7.6$ MGOe and $H_{\text{cj}} = 5.81$ kOe were achieved by melt-spun (MM)_{12.5}Fe_{78.9}B_{8.6} alloys. After die-upset, the $(BH)_{\max}$ and H_{cj} of MM_{12.5}Fe_{78.9}B_{8.6} alloys change to 4.1 MGOe and 1.75 kOe, respectively.⁹ In this work, conventional sintering method was applied for preparation of MM₁₄Fe_{79.9}B_{6.1} magnet. The relationship between magnetic properties and sintering temperature has been researched. Microstructure of sintered magnets and the change of elements in grains are also explored.

II. EXPERIMENTAL

With nominal compositions of MM₁₄Fe_{79.9}B_{6.1} (at. %) alloy was prepared by arc-melting in argon atmosphere. The ingot was melted five times to ensure homogenization in a vacuum furnace.

^aCorresponding author: B. G. Shen (shenbaogen@yeah.net)

The purpose of the ingot is to study the lattice constants and the theoretical density of $\text{MM}_2\text{Fe}_{14}\text{B}$ phase.

The powders of $\text{MM}_{14}\text{Fe}_{79.9}\text{B}_{6.1}$ (at. %) alloy were prepared by induction melting, subsequent strip-casting (SC), hydrogen decrepitating (HD) and jet-milling (JM). The average particle size of the powders was approximately 3.0 μm . Then the powders were aligned and compacted under a magnetic field of 1.8 T and a pressure of ~ 5 MPa in a N_2 -filled glove box, followed by an isostatic pressing at ~ 160 MPa. The green compacts were sintered for 2 h at different temperatures from 1000 to 1080 $^\circ\text{C}$, followed by a two-step tempering treatment, which was performed for 2 h at 900 $^\circ\text{C}$ and for 2 h at 520 $^\circ\text{C}$, respectively.

The density of the magnets was measured based on Archimedes principle. The magnetic properties, including B_r , H_{cj} , and $(BH)_{\text{max}}$, were measured by quasi-closed loop permanent magnetic measurement system NIM-500C. The phase component of the magnets were characterized by X-ray diffraction (XRD) using a Rigaku D/Max-2400 diffractometer with $\text{Cu K}\alpha$ radiation. Curie temperature was measured by vibrating sample magnetometer (Model 4 HF-VSM). The microstructure was examined and characterized by a Phenom ProX scanning electron microscope (SEM) equipped with an energy dispersive X-ray spectroscopy (EDS).

III. RESULTS AND DISCUSSION

Theoretical pattern was simulated by means of GSAS program for $\text{MM}_{14}\text{Fe}_{79.9}\text{B}_{6.1}$ ingot. The crystal parameter of refinement for the $\text{MM}_{14}\text{Fe}_{79.9}\text{B}_{6.1}$ sample were referred from the single crystal data of $\text{Nd}_2\text{Fe}_{14}\text{B}$ (JCPDS PDF#39-0437). The lattice constants of $\text{MM}_2\text{Fe}_{14}\text{B}$ were determined to be $a = b = 8.780$ \AA , $c = 12.185$ \AA . The fraction factors and thermal vibration parameters were refined with convergence and satisfied the reflection condition, $R_{\text{wp}} = 11$ %, $\text{CHI}^{**2} = 1.05$ %, $\text{Nbos} = 7.9$ %. The result show that the lattice constants of $\text{MM}_2\text{Fe}_{14}\text{B}$ are smaller than that of $\text{Nd}_2\text{Fe}_{14}\text{B}$ ($a = b = 8.792$ \AA , $c = 12.27$ \AA).¹⁰ Changes of rare earth cations in the host lattice might be the reason for the result. Specifically, a part of positions of Nd^{3+} were occupied by both Ce^{3+} and Ce^{4+} ions, and the radius of Ce^{4+} ion is small compared with Nd^{3+} , which led to the decrease of lattice constants.¹¹ Meanwhile, the theoretical density of $\text{MM}_2\text{Fe}_{14}\text{B}$ magnet ($\rho = 7.589$ g/cm^3) was also obtained by XRD refinement.

Fig. 1 shows XRD patterns for the anisotropic sintered $\text{MM}_{14}\text{Fe}_{79.9}\text{B}_{6.1}$ magnets. The intensity of (004), (105), (006) and (008) peaks are enhanced. It confirms that all samples contain the anisotropic $\text{R}_2\text{Fe}_{14}\text{B}$ structure phase. The alignment degree estimated by the intensity ratio I_{006}/I_{105} have almost no change when the sintering temperature increased from 1010 $^\circ\text{C}$ to 1060 $^\circ\text{C}$.

In order to ascertain the Curie temperature of the sintered $\text{MM}_2\text{Fe}_{14}\text{B}$ magnet, its magnetization dependent on temperature was measured at the magnetic field 500 Oe and under the increasing temperature from 27 $^\circ\text{C}$ to 287 $^\circ\text{C}$. The curves of magnetization and dM/dT dependent on temperature are shown in Fig. 2. It can be obviously seen that the Curie temperature of the sintered $\text{MM}_2\text{Fe}_{14}\text{B}$

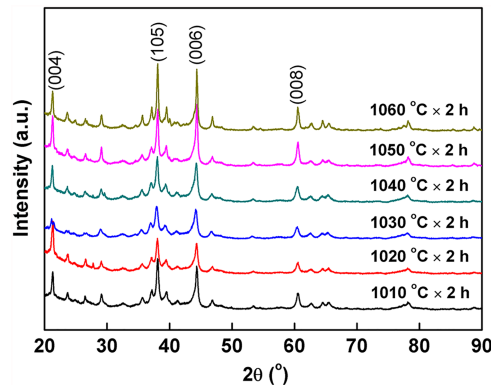


FIG. 1. XRD patterns of the anisotropic $\text{MM}_{14}\text{Fe}_{79.9}\text{B}_{6.1}$ magnets sintered at different conditions.

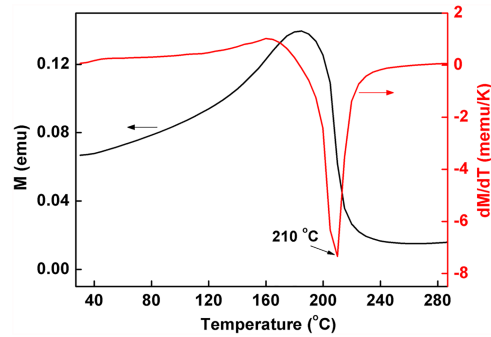


FIG. 2. Temperature dependence of magnetization and dM/dT of the sintered magnet at 1010 °C.

magnet was about 210 °C, which is lower than that of $\text{Nd}_2\text{Fe}_{14}\text{B}$ ($T_c = 312$ °C). According to the literatures, the Curie temperature of $\text{La}_2\text{Fe}_{14}\text{B}$, $\text{Ce}_2\text{Fe}_{14}\text{B}$ and $\text{Pr}_2\text{Fe}_{14}\text{B}$ is 257 °C, 157 °C and 292 °C, respectively.¹² $\text{MM}_2\text{Fe}_{14}\text{B}$'s Curie temperature is higher than $\text{Ce}_2\text{Fe}_{14}\text{B}$'s and lower than the others. Curie temperature of R-Fe-B is mainly determined by the exchange interaction of Fe-Fe atom pair, the close distance between Fe-Fe would weaken their exchange interaction and then cause the reduction of Curie temperature.¹³ Massive Ce^{4+} ions substitution for Nd^{3+} in $\text{MM}_{14}\text{Fe}_{79.9}\text{B}_{6.1}$ magnets, the distances between Fe-Fe get close due to the smaller radius of Ce^{4+} compared with Nd^{3+} . This point can also be seen from the decrease of lattice constants of $\text{MM}_2\text{Fe}_{14}\text{B}$. Consequently, a sharp decrease of T_c was probably due to the existence of Ce^{4+} . One can find the M was not reduced to zero when the temperature exceeded 240 °C, it suggests that some soft magnetic phase may exist in the sintered $\text{MM}_2\text{Fe}_{14}\text{B}$ magnets.¹⁴ It may be produced in the process of strip casting, soft magnetic phase will deteriorate the intrinsic coercivity and maximum energy product of magnets. Therefore, optimizing the strip casting technique in order to restrain the production of soft magnetic phase is helpful to improve the performance of the magnet.

The magnetic properties and density of the $\text{MM}_{14}\text{Fe}_{79.9}\text{B}_{6.1}$ magnets with different sintering and tempering temperatures are compared in Fig. 3. According to Fig. 3 (a) and (b), the corresponding

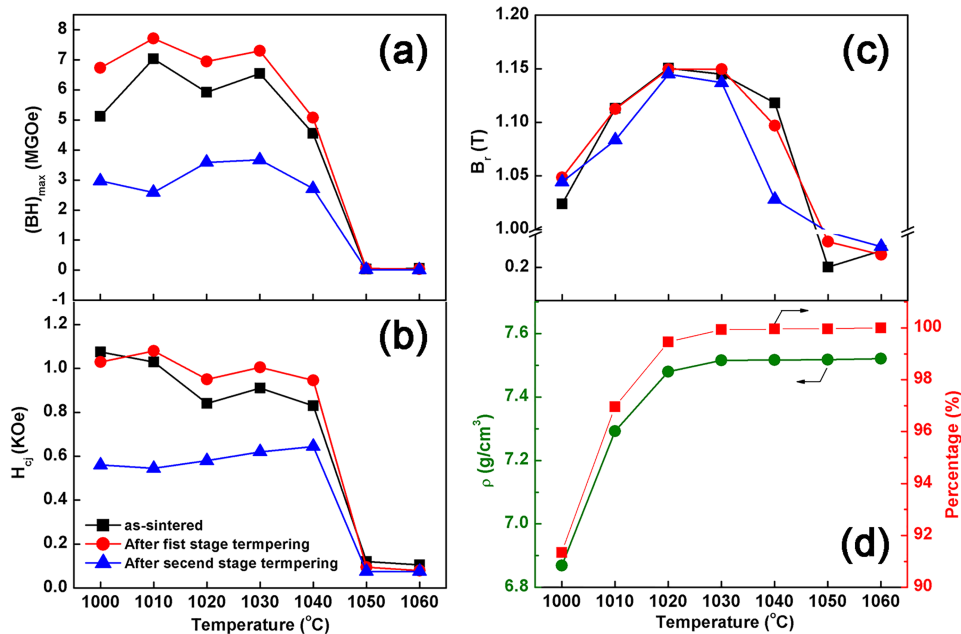


FIG. 3. Effects of the sintering and tempering temperature on maximum energy product (a), intrinsic coercive force (b), remanence (c), and density (d) of the $\text{MM}_{14}\text{Fe}_{79.9}\text{B}_{6.1}$ magnet.

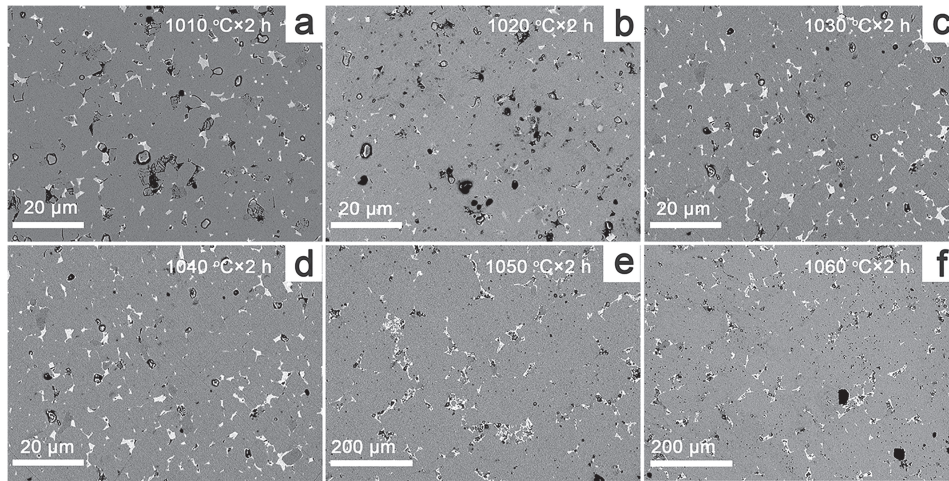


FIG. 4. SEM-back scattered micrographs of the $\text{MM}_{14}\text{Fe}_{79.9}\text{B}_{6.1}$ magnets after two stage tempering under different sintering temperatures.

$(BH)_{\text{max}}$ and H_{cj} have no significant change with the increase of sintering temperature from 1000 °C to 1030 °C. But they decreased drastically when the sintering temperature exceeded 1040 °C. The B_{r} was basically first increased and then decreased in Fig 3. (C). With increase of the sintering time, liquid phase decreased and grains were getting close to others, solid phase sintering occurred on the contact surfaces of grains, the result was that the grains grew very large and the grain boundaries disappeared.¹⁵ This will adversely affect the performance of the magnet. The $(BH)_{\text{max}}$ and H_{cj} increased slightly after the first stage of tempering at 900 °C, it was due to the optimization of grain boundaries.¹⁶ But, both of them dropped almost in half after the second stage of tempering at 520 °C. This is mainly because of deterioration of the grain boundaries. The maximum value of $(BH)_{\text{max}} = 7.6$ MGOe and $H_{\text{cj}} = 1080$ Oe was obtained when sintered at 1010 °C and tempering at 900 °C, respectively. Fig. 3 (d) shows the density and its normalization of the magnets sintered at different temperatures. It can be seen that a rapid increase in the density from 91.2 % to 99.9 % when the sintering temperature increased from 1000 °C to 1030 °C, the corresponding density value increased from 6.85 g/cm³ to 7.52 g/cm³. The density was not changed with the increase of sintering temperature from 1030 °C to 1060 °C. It means the magnet was densification when sintering temperature reached 1030 °C.

Fig. 4 shows the SEM micrographs in backscatter mode for $\text{MM}_{14}\text{Fe}_{79.9}\text{B}_{6.1}$ magnets after two stage tempering under different sintering temperatures. There were no obviously continuous grain boundaries and change of grain size at lower sintering temperature from 1010 °C to 1040 °C. Comparably, the grain size grew very large (>200 μm) when the sintering temperature increased to 1050 °C. Due to the differences of the formation energy and technical conditions for R-Fe-B (R= La, Ce, Pr and Nd), the atomic ratio of La, Ce, Pr and Nd in the grains of the sintered $\text{MM}_{14}\text{Fe}_{79.9}\text{B}_{6.1}$ magnets was not the same. The mean percentages of La, Ce, Pr and Nd in the grains by means of EDS analysis were summarized in Table I. Compared with misch metal, the percentages of Ce and Pr only have a small change and almost don't vary with sintering temperature. And it also can be clearly seen that the percentage of La reduces by ~ 7.5 at. %, which is almost equal to the increased

TABLE I. EDS analysis of the mean percentages of La, Ce, Pr and Nd in the grains of the $\text{MM}_{14}\text{Fe}_{79.9}\text{B}_{6.1}$ magnets in Fig. 4.

Sample	La (at. %)	Ce (at. %)	Pr (at. %)	Nd (at. %)
1020 °C × 2 h	~ 20.28	~ 51.94	~ 5.21	~ 22.48
1040 °C × 2 h	~ 21.50	~ 50.35	~ 5.27	~ 23.10
1060 °C × 2 h	~ 19.83	~ 51.08	~ 5.15	~ 23.96
Misch metal	~ 28.00	~ 52.00	~ 5.10	~ 14.70

percentage of Nd. That is mainly because La-Fe-B need very rigorous technical condition to form the 2: 14: 1 phase compared with Ce-Fe-B, Pr-Fe-B and Nd-Fe-B, and $\text{La}_2\text{Fe}_{14}\text{B}$ phase is unstable.¹⁷ The reduced La, in the form of its oxide, existed in the grain boundary phase.¹⁸

IV. CONCLUSION

The $\text{MM}_{14}\text{Fe}_{79.9}\text{B}_{6.1}$ magnets were prepared by conventional sintering method. $\text{R}_2\text{Fe}_{14}\text{B}$ structure phase was confirmed by XRD patterns. Its crystal parameter and theoretical density are small compared with $\text{Nd}_2\text{Fe}_{14}\text{B}$. The Curie temperature of the sintered $\text{MM}_2\text{Fe}_{14}\text{B}$ magnet was about 210 °C, that's maybe because the existence of Ce^{4+} ions weakened Fe-Fe exchange interaction. When the sintering temperature reached 1030 °C, the magnet was densification. The optimum $(BH)_{\text{max}}$ of 7.6 MGOe and H_{cj} of 1080 Oe was obtained when sintered at 1010 °C for 2 h and tempering at 900 °C for 2h. When the sintering temperature increased to 1050 °C, solid phase sintering occurred on the contact surfaces of grains, the grain size grew very large and magnetic properties sharply declined. In the grains, the percentage of La reduced by ~ 7.5 at. %, that's because rigorous technical condition should be required for forming $\text{La}_2\text{Fe}_{14}\text{B}$ phase. It might make to further improve the performance of $\text{MM}_{14}\text{Fe}_{79.9}\text{B}_{6.1}$ by modifying SC process.

ACKNOWLEDGMENTS

This work was supported by the National Key Research Program of China (Grant Nos. 2014CB643702, 2016YFB0700903), the National Natural Science Foundation of China (Grant No. 51590880) and the Knowledge Innovation Project of the Chinese Academy of Sciences (Grant No. KJZD-EW-M05).

- ¹ M. Zhang, Z. B. Li, B. G. Shen, F. X. Hua, and J. R. Sun, *J. Alloys Compd.* **651**, 144 (2015).
- ² Z. B. Li, B. G. Shen, M. Zhang, F. X. Hu, and J. R. Sun, *J. Alloys Compd.* **628**, 325 (2015).
- ³ M. Hussain, J. Liu, L. Z. Zhao, X. C. Zhong, G. Q. Zhang, and Z. W. Liu, *J. Magn. Magn. Mater.* **399**, 26 (2016).
- ⁴ W. Gong and G. C. Hadjipanayis, *J. Appl. Phys.* **63**, 3513 (1988).
- ⁵ J. M. D. Coey, *J. Magn. Magn. Mater.* **248**, 441 (2002).
- ⁶ Z. D. Zhang, W. Liu, J. P. Liu, and D. J. Sellmyer, *J. Phys. D: Appl. Phys.* **33**, 217 (2000).
- ⁷ J. Fidler, T. Schrefl, S. Hoefinger, and M. Hajduga, *J. Phys.: Condens. Matter* **16**, 455 (2004).
- ⁸ S. Sugimoto, *J. Phys. D: Appl. Phys.* **44**, 064001 (2011).
- ⁹ K. Y. Ko, S. Yoon, and J. G. Booth, *J. Magn. Magn. Mater.* **176**, 313 (1997).
- ¹⁰ J. F. Herbst, J. J. Croat, F. E. Pinkerton, and W. B. Yelon, *Phys. Rev. B* **29**, 4176 (1984).
- ¹¹ A. Alam and D. D. Johnson, *Phys. Rev. B* **89**, 235126 (2014).
- ¹² E. Burzo, *Rep. Prog. Phys.* **61**, 1099 (1998).
- ¹³ S. Hirosawa, Y. Matsuura, H. Yamamoto, S. Fujimura, M. Sagawa, and H. Yamauchi, *J. Appl. Phys.* **59**, 873 (1986).
- ¹⁴ G. H. Yan, R. J. Chen, Y. Ding, S. Guo, D. Lee, and A. R. Yan, *J. Phys.: Conf. Ser.* **266**, 012052 (2011).
- ¹⁵ B. E. Davies, R. S. Mottram, and I. R. Harris, *Mater. Chem. Phys.* **67**, 272 (2001).
- ¹⁶ X. L. Liu, T. Y. Ma, X. J. Wang, and M. Yan, *J. Magn. Magn. Mater.* **382**, 26 (2015).
- ¹⁷ G. C. Hadjipanayis, *Can. J. Phys.* **65**, 1200 (1987).
- ¹⁸ X. F. Zhang, Y. Shi, Q. Ma, Y. L. Liu, M. F. Shi, Y. F. Li, G. F. Wang, and Z. R. Zhao, *Rare Metal Mat. Eng.* **44**, 748 (2015).